Vol. 749: 141–158, 2024
https://doi.org/10.3354/meps14720

MARINE ECOLOGY PROGRESS SERIES
Mar Ecol Prog Ser

Published November 21

Shifting temperature–abundance relationship for Bering Sea walleye pollock consistent with northward expansion during exceptionally warm conditions

Krista B. Oke[1,3,*], Michael A. Litzow[2], Franz Mueter[1]

[1]College of Fisheries and Ocean Sciences, University of Alaska Fairbanks, 17101 Point Lena Loop Road, Juneau, Alaska 99801, USA
[2]Alaska Fisheries Science Center, NOAA Fisheries, 301 Research Ct., Kodiak, Alaska 99615, USA

[3]*Present address:* Fisheries, Aquatic Science, and Technology (FAST) Laboratory, Alaska Pacific University and Alaska Fisheries Science Center, NOAA Fisheries, 17109 Point Lena Loop Road, Juneau, Alaska 99801, USA

ABSTRACT: Rapid climate change in high-latitude ecosystems presents a challenge to fisheries management, as ecosystems are exposed to novel climate conditions that might expose non-stationary climate–biology relationships. Recently, the eastern Bering Sea has experienced a series of warm years outside the range of previous observations, resulting in shifting species distributions. We tested whether exceptionally warm temperatures from 2014–2019 revealed temporal non-stationarity in the relationship between temperature and the local abundances of walleye pollock *Gadus chalcogrammus*, an ecologically and commercially important species. Using survey catch per unit effort (CPUE) as a local abundance proxy, we detected a gradual shift through time in the local abundance–bottom temperature relationship, but little evidence for a sharp transition associated with marine heatwave conditions. Because pollock have expanded their range into novel habitats in the northeast Bering Sea (NEBS), we tested whether our models, parameterized for the southeast Bering Sea (SEBS), had predictive skill in the northeast. Our models were generally able to identify areas of high and low CPUE, though they under-predicted the magnitude of abundance observed in the northeast during the warm years. Spatial associations between pollock and other species differed between the warm period (2014–2019) and previous decades (1982–2013) for 3 of 9 species, providing mixed evidence for non-stationarity. These findings contrast with results showing sharp rather than gradual changes in climate–biology relationships associated with climate transitions in nearby ecosystems. The same processes that govern walleye pollock abundance and distribution appear to apply to both the SEBS, historically the core of their distribution, and the NEBS.

KEY WORDS: Bering Sea · Pollock · Non-stationarity · Rapid warming

1. INTRODUCTION

Rapid climate change in high-latitude ecosystems presents a profound challenge for our understanding of ecosystem dynamics. High northern latitudes are experiencing rapid warming, including the Bering Sea (Danielson et al. 2020), which has recently experienced major shifts in community composition associated with high temperatures that are unprecedented in climate records (Grebmeier et al. 2006, Huntington et al. 2020). Evidence is also mounting that many climate–biology relationships in the North Pacific might be non-stationary (Litzow et al. 2018, 2019, Wainwright 2021). Non-stationary relationships, which occur when the relationship between 2 (or more) variables changes through time, might be revealed as high-latitude regions enter novel climate states due to anthropogenic climate change (Williams & Jackson 2007). Non-stationarity would compound the challenges of responding to climate change for management and con-

*Corresponding author: kristaoke@gmail.com

Publisher: Inter-Research · www.int-res.com

servation, as it would imply a loss of predictive skill for models based on existing ecological knowledge.

Rapid climate change is of particular concern in the Bering Sea region, which supports some of the largest single-species fisheries in the world. Beginning in 2013–2014, a marine heatwave and subsequent extended warm period have exposed the Bering Sea ecosystem to a previously unobserved set of climate conditions (Di Lorenzo & Mantua 2016, Huntington et al. 2020). This marine heatwave has been formally attributed to anthropogenic radiative forcing (Walsh et al. 2018, Laufkötter et al. 2020). In response, many species have shifted their distributions (Stevenson & Lauth 2019), with several commercially important species moving northward from the southeastern Bering Sea (SEBS) to the northeastern Bering Sea (NEBS) (Stevenson & Lauth 2019, Thorson et al. 2019, Marsh et al. 2020, O'Leary et al. 2020). Much of our biological understanding of eastern Bering Sea (EBS) population and community dynamics was developed prior to the current extended warm period. The extent to which this understanding will or will not hold under novel climates remains unknown (Williams & Jackson 2007). Given that 2014–2019 climate conditions are novel among contemporary climate records, the question can be raised whether non-stationary relationships between climate variables and community composition might result. Non-stationarity in the relationships that govern population and community dynamics would complicate the interpretation of population projections for research and management purposes.

Walleye pollock *Gadus chalcogrammus* (henceforth referred to as pollock) landings are among some of the highest landings globally of any fish species (FAO 2023). Bering Sea pollock support the largest fishery in the United States by volume, with a 2019 catch of 1.41 million tons, and first-wholesale value of US $1.55 billion (Ianelli et al. 2020). Traditionally, pollock have occurred at very high abundances in the SEBS but only at very low abundances in the NEBS (Stevenson & Lauth 2019). Pollock are targeted by the fishery in the SEBS but not the NEBS. In the SEBS, pollock are not only a dominant species in terms of commercial catch but also in terms of the influence they exert on the ecosystem, in large part due to their high abundances and their ecological role as both an important forage fish and a predator (Aydin & Mueter 2007). Pollock recruitment and abundances are influenced by many factors, including fishing, predator and prey densities (Ciannelli et al. 2002, Hunt et al. 2011), age-class dynamics (Thorson et al. 2017, Ianelli et al. 2018), and environmental conditions (Hunt et al. 2011). In particular, pollock distribution is shaped by the annual extent of sea ice and the cold pool, or the area of bottom temperature below 2°C in the Bering Sea, which adult pollock tend to avoid (Kotwicki et al. 2005, Mueter & Litzow 2008, Kotwicki & Lauth 2013).

Warm temperatures since 2014 have coincided with an exceptionally small or absent cold pool in the SEBS and a remarkably rapid distributional shift of pollock from the SEBS into the northern Bering Sea in both US and Russian waters (Eisner et al. 2020, O'Leary et al. 2020). Relatively high abundances of pollock have been detected in areas of the NEBS since 2017, whereas surveys in 2010 and earlier generally found low pollock abundances (Stevenson & Lauth 2019). Previous studies have shown that including cold pool extent and/or bottom temperature in models of pollock abundance and distribution improves model performance (e.g. Thorson 2019, O'Leary et al. 2020). However, whereas previous studies have investigated non-linear and/or spatially varying responses to cold pool and bottom temperature, the associations with cold pool and bottom temperature are typically considered to be temporally stationary — i.e. that a single temperature–pollock relationship pertains throughout the observational period.

The unprecedented climate conditions and pollock distributions observed in recent years raise the question of whether pollock are responding to novel conditions in a previously unobserved manner. Warmer temperatures result in higher metabolic demands and thus higher prey requirements (Brown et al. 2004) which could alter foraging behavior. Increasing temperatures could also alter habitat suitability, especially if preferred temperatures become uncoupled from otherwise preferred habitat features. Current efforts to fit environmentally dependent species distribution models (SDMs) to historical data or to project future distribution changes in pollock generally assume stationary relationships with temperature (Thorson et al. 2017, Alabia et al. 2018, Thorson 2019). However, SDMs parameterized with observational data are known to be vulnerable to failure when deployed out of sample (Araujo & New 2006, Williams & Jackson 2007, Urban et al. 2016), in particular if underlying relationships with climate prove to be non-stationary (Fitzpatrick & Hargrove 2009, Veloz et al. 2012, Urban et al. 2016). Furthermore, recent SDMs have revealed important changes in distributions in response to climate or between cold and warm periods in the EBS (Thorson et al. 2017, Alabia et al. 2018, Thorson 2019), but the potential for novel climate conditions to arise in the future could limit the utility of historic data to predict future distributions.

As pollock distributions respond to novel climate conditions, so might the distributions of their prey, competitors, and predators, which could result in different microhabitats being favored. Shifting patterns of species overlap and changing strengths of species interactions can both provide a further source of error for SDMs (Urban et al. 2012, 2016). Already there is evidence that warmer temperatures and reduced cold pool extent can negatively influence pollock recruitment by increasing the extent of overlap with predators (Hunsicker et al. 2013, Spencer et al. 2016, Uchiyama et al. 2020, Thorson et al. 2021) while reducing the extent of overlap with prey (Siddon et al. 2013). In addition, evidence from invasion biology has shown that dispersers and individuals at the leading edge of expanding ranges often have important phenotypic differences compared to individuals near the core distribution that can alter their ecological interactions and impacts (Cote et al. 2017, Pinsky et al. 2020). It is possible that the pollock that moved into the NEBS could differ in their habitat preferences or behavior compared to those that stayed in the SEBS. Given that marine heatwaves similar to the 2013–2015 event are predicted to occur more frequently with climate change (Frölicher et al. 2018, Oliver et al. 2018, Laufkötter et al. 2020), we sought to determine whether the 2013–2015 heatwave in the North Pacific and subsequent warm period in the Bering Sea corresponded to a fundamental shift in the relationship between pollock abundance and temperature or interactions between pollock and other species.

The overarching goal of our study was to investigate whether recent (2014–2019) unprecedented warm temperatures in the EBS represent a new climate envelope in which knowledge of pollock dynamics and species interactions gained under past climate conditions might no longer be predictive. In particular, our first objective was to determine whether the relationship between local pollock abundance and bottom temperature in the SEBS has changed in the warm 2014–2019 period relative to the 1982–2013 period. Next, we turned to the NEBS, where 2014–2019 climate conditions were more typical of those in the SEBS during previous decades, but where different habitats or species interactions might result in fundamentally different responses to bottom temperature. Thus, to investigate whether our understanding of pollock distributions from the SEBS will hold in the NEBS, our second objective was to assess the ability of models of local pollock abundance fit to data from the SEBS to predict pollock abundance in the NEBS. Different age classes of pollock tend to have different spatial and vertical distributions (Kotwicki et al. 2005, 2015). Thus, our third objective was to determine whether the local abundances of different size classes responded differently to warm temperatures in the warm 2014–2019 period. Finally, the potential for different species to respond to warming in different ways, or to encounter new species as they shift northwards, could result in shifting species interactions. Our fourth objective was to evaluate the evidence for non-stationarity in spatial associations between the local abundance of pollock and the abundances of other common species in the SEBS.

2. MATERIALS AND METHODS

2.1. Study system

The EBS (Fig. 1) is characterized by a large, shallow shelf subject to nutrient-rich currents flowing northward over the shelf and exiting through the Bering Strait into the Chukchi Sea (for a general review of the EBS ecosystem, see Aydin & Mueter 2007). The SEBS is characterized by strong cross-shelf gradients defined by bathymetry and water column structure that are dominant drivers of the biogeography of fish on the shelf (Mueter & Litzow 2008). Similar cross-shelf gradients are evident on the northern Bering Sea shelf but their impact on fish distributions in this region is poorly understood. For the purposes of our study, we distinguish between SEBS and NEBS (Fig. 1).

The EBS supports some of the largest fisheries in the United States and includes economically important stocks of pollock, Pacific salmon *Oncorhynchus* spp., crabs (e.g. *Chionoecetes* spp. and *Paralithodes* sp.), and flatfishes (e.g. yellowfin sole *Limanda aspera*). The ecology of the EBS ecosystem is dominated by demersal fishes and in particular has been dominated by pollock since the 1980s (Aydin & Mueter 2007). The region encompasses the boundary between the sub-Arctic and Arctic ecoregions where species from both ecoregions mix (Aydin & Mueter 2007, Mueter & Litzow 2008). The EBS is strongly influenced by seasonal ice cover and a persistent cold pool of bottom temperatures below 2°C, the extent and timing of both of which exert strong ecosystem influence and vary greatly among years (Walsh & Johnson 1979, Aydin & Mueter 2007). However, the years 2014–2019 were characterized by unprecedented warm temperatures, low sea ice extent, and low or non-existent cold pool extent (Di Lorenzo & Mantua 2016, Duffy-Anderson et al. 2019, Danielson et al. 2020, Huntington et al. 2020, Rohan et al. 2022). These rapid changes have led to broad-scale shifts in

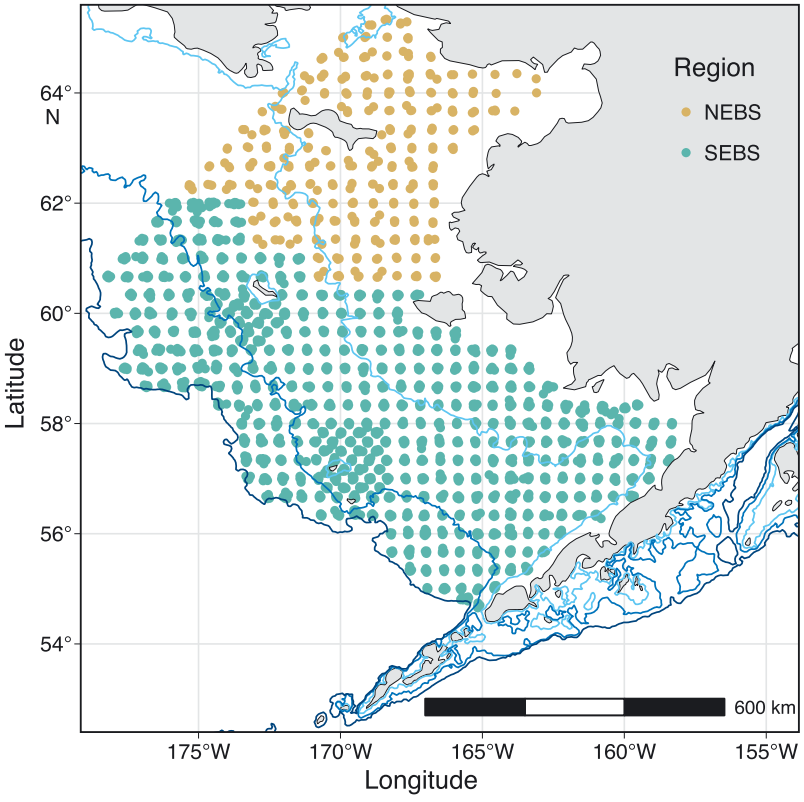

Fig. 1. Study area, with sampling events from northeast Bering Sea (NEBS) and southeast Bering Sea (SEBS) sites. The bottom trawl survey samples a standard grid of stations each year, so sampling events from different years but the same station tend to cluster tightly in space. The 50 m (light blue), 100 m (blue), and 200 m (dark blue) depth contours are indicated

species distributions (Alabia et al. 2018, Stevenson & Lauth 2019, Eisner et al. 2020, O'Leary et al. 2020) and an increasing dominance of sub-Arctic taxa in the EBS (Mueter & Litzow 2008).

2.2. Bottom trawl survey data

The pollock data used in this study come from the annual bottom trawl surveys of the SEBS conducted by the National Oceanic and Atmospheric Administration (NOAA) National Marine Fisheries Service (NMFS) Alaska Fisheries Science Center (AFSC) Groundfish Assessment Program (GAP). The bottom trawl data provide estimates of the abundance and biomass of demersal species within the survey region, including the demersal portion of the EBS pollock stock. In addition, in certain years, GAP extended the bottom trawl survey into the NEBS following the SEBS survey. Both surveys use the same methodology as summarized in annual reports published by NOAA (e.g. Lauth et al. 2019). In the SEBS, 376 fixed stations on a 20 × 20 nautical mile (nmi) (37 × 37 km) grid are sampled each year by an 83-112 eastern bottom trawl (83 ft [25 m] headrope and 112 ft [34 m] footrope). Sampling in the NEBS has been more opportunistic and occurred with less consistent schedules and stations, but has been conducted using the same gear, vessels, and design as in the SEBS. Triennial surveys from 1982–1991 sampled portions of the NEBS along a 40 × 40 nmi (74 × 74 km) grid. In 2010 and again in 2017, 2019, and 2021, the NEBS was sampled as an extension of the standard 20 × 20 grid in the SEBS. An emergency survey was conducted in the NEBS in 2018 along a 30 × 30 nmi (55.6 × 55.6 km) grid in response to decreased abundances in the SEBS. We downloaded SEBS and NEBS bottom trawl survey data for years 1982–2021 from the online RACEBASE archive (https://www.fisheries.noaa.gov/foss/f?p=215:28), which assigns non-standard stations to the name of the nearest standard station (Kearney 2021). We excluded stations from the 10 × 10 nmi (18.5 × 18.5 km) grid sampled in Norton Sound in the 1980s because this grid has not been sampled recently.

The bottom trawl survey is conducted for monitoring and assessment purposes, hence methods are standardized as much as possible across stations and years to ensure that catch per unit effort (CPUE, swept area estimate of biomass per unit area in kg ha^{-1}) can be directly compared across time and space. As a metric of relative abundance for our analyses, we natural-log-transformed CPUE after adding a small constant (log(CPUE + 1)) to achieve approximate normality of model residuals and to account for occasional zeros. In addition to the CPUE data described above, we were also interested in CPUE by size class. Data on CPUE binned by sex and total length (in 1 cm bins) were obtained for years 1982–2019 from a query of RACEBASE (Table S1 in the Supplement at www.int-res.com/articles/suppl/m749p141_supp.pdf).

2.3. Community data

In addition to pollock, we selected several species that may interact with pollock to investigate whether

correlations among pollock and these species have shifted in the recent warm period (Objective 4, see Section 1). We focused on species that are commonly detected in the bottom trawl survey and that are expected to interact with pollock as competitors or predators based on a review of the pollock literature. These species included: Alaska plaice *Pleuronectes quadrituberculatus*, arrowtooth flounder *Atheresthes stomias*, flathead sole *Hippoglossoides elassodon*, Pacific cod *Gadus macrocephalus*, Pacific halibut *Hippoglossus stenolepis*, rock sole *Lepidopsetta* spp., snow crab *Chionoecetes opilio*, Tanner crab *C. bairdi*, and yellowfin sole *Limanda aspera*.

2.4. Haul-specific environmental data

We were primarily interested in the effects of bottom temperatures on the spatial distribution of pollock but also considered several spatial covariates recorded during each haul of the bottom trawl survey, including latitude, longitude, and bottom depth. Latitude and longitude coordinates were converted to reflect actual distances using the equal-distance Albers projection via the function 'mapproject' in the mapproj package version 1.2.7 (McIlroy et al. 2020). We excluded any individual hauls that were sampled at depths greater than 180 m because they are rare in the dataset (n = 24 hauls) and are beyond the typical bottom depths inhabited by pollock. Bottom temperature (°C) was not recorded for a small subset of SEBS hauls (524/14 023 records). To fill in these missing values, we constructed general additive models (GAMs) of bottom temperature with a non-linear smoothed effect of bottom depth and a tensor product interaction between latitude and longitude. Each year was modeled separately and R^2 values were generally high (ranging from 0.623 to 0.893). Based on the recorded bottom depth and coordinates of the hauls with missing temperature data, we replaced missing values with predicted bottom temperatures from these models.

2.5. Statistical analyses

The main question we aimed to address was whether the relationship between local pollock abundance (using CPUE as a proxy) and bottom temperature changed in the warm 2014–2019 period relative to the 1982–2013 period. To test this, we followed an information-theoretic approach and compared 4 generalized additive mixed models (GAMMs) that reflect alternative hypotheses about the response of pollock to local temperatures based on *a priori* understanding of pollock ecology. The 4 models differed primarily in how temperature affects CPUE, with other model structure held constant across models. We then assessed the relative strength of evidence for our competing hypotheses.

Model 1: non-linear response model. This was our base model allowing for a non-linear response to local bottom temperatures, based on the following parameterization:

$$Y_{t,i} = \alpha + a_t + f_1(z_{t,i}) + f_2(BT_{t,i}) + \varepsilon_{t,i} \quad (1)$$

where $Y_{t,i}$ is log(CPUE + 1) at station i in year t, α is the overall intercept, and a_t is a random year effect to account for interannual variability in average CPUE and the resulting lack of independence of samples taken within the same year. The smooth function $f_1(z_{t,i})$ is a smoothed effect of bottom depth (z_i) to account for the fact that pollock tend to aggregate on deeper portions of the shelf, particularly near the 100 m isobath (Kotwicki et al. 2005). Local bottom temperature is included as a smoothed effect, $f_2(BT_{t,i})$. We fit bottom temperature as a nonlinear effect rather than a linear effect because preliminary analyses and some previous studies (Thorson 2019, Grüss et al. 2020) suggest that the effect of bottom temperature on pollock density is non-linear, likely reflecting a preference for intermediate temperatures, and because there is no *a priori* reason to assume a linear response. We limited the flexibility of the smooth term to 3 effective degrees of freedom (basis dimension k = 4 for smooth term) because we considered a more complex response to be biologically unrealistic. In addition, we accounted for potential spatial autocorrelation in the residuals, $\varepsilon_{t,i}$, using an exponential spatial correlation structure that assumes that, within a given year, residual correlations among stations decay exponentially with distance. Other correlation structures, including Gaussian, spherical, and rational quadratic spatial correlations, were explored but provided worse fits. We used this approach because we were primarily interested in the mean response to temperature, but needed to account for any remaining spatial autocorrelation in the residuals.

Model 2: non-stationary non-linear response. This model accounts for possible non-stationarity by allowing for a separate non-linear relationship between pollock CPUE and bottom temperature in the warm 2014–2019 period compared to the 1982–2013 period. This model retains the same structure as the non-linear model, but updates the $BT_{t,i}$ term to allow for different temperature responses by period (p), modeled as a factor smooth interaction

between bottom temperature and period (1982–2013 versus 2014–2019):

$$Y_{t,i} = \alpha + a_t + f_1(z_{t,i}) + f_2(BT_{t,i}, p) + \varepsilon_{t,i} \quad (2)$$

Model 3: non-stationary linear response. This model assumes a linear response to local temperatures whose magnitude and/or sign may differ between periods to account for possible non-stationarity. This model is similar to Model 2 but uses a linear interaction between period and bottom temperature:

$$Y_{t,i} = \alpha + a_t + f_1(z_{t,i}) + \beta_p \times BT_{t,i} + \varepsilon_{t,i} \quad (3)$$

where β_p is a slope that is specific to each period (early: 1982–2013; late: 2014–2019) and is modeled as an interaction between $BT_{t,i}$ and a categorical variable for period. For both the non-stationary non-linear and non-stationary linear models, we would interpret a significant interaction between bottom temperature and period to indicate a non-stationary relationship between CPUE and bottom temperature associated with the onset of unusually warm temperatures in the late period.

Model 4: time-varying model. The final model allowed the response to temperature to change through time using a tensor product interaction between bottom temperature and year. This model is the most flexible, allowing the bottom temperature–CPUE relationship to change smoothly over time, rather than a one-time change at the onset of the 2014–2019 warm period. Specifically:

$$Y_{t,i} = \alpha + a_t + f_1(z_{t,i}) + f_2(BT_{t,i}, t) + \varepsilon_{t,i} \quad (4)$$

where t is year. The bottom temperature-by-year interaction was implemented using a 't2' tensor-product smooth.

We compared the 4 models described above using the Akaike information criterion (AIC) and Akaike weights (Burnham & Anderson 2002) to assess the relative strength of evidence for our competing hypotheses. We excluded data from stations that had been sampled in fewer than 5 years and from any station that is considered to be part of the NEBS. To address concerns regarding collinearity of covariates, correlations among covariates (bottom depth and bottom temperature) were assessed to confirm that they did not exceed $|r| = 0.5$. Distributions of residuals are provided in Fig. S1. As an additional measure of model fit, we performed leave-one-out cross validation by dropping 1 year of data, fitting each model to the remaining years of data, and then predicted log(CPUE + 1) for all values in the missing year. Within-sample predictive ability was assessed using root mean square error (RMSE).

A potential challenge for our modeling efforts arises from the fact that the early and late periods differed in their overall climate patterns: bottom temperatures observed in the late period were generally warmer than those observed in the early period, consistent with the observed pattern of warming in the Bering Sea (Walsh et al. 2018, Duffy-Anderson et al. 2019). Consequently, there was limited overlap between the range of temperatures observed within each period such that period-specific temperature effects (Models 2 and 3) could be strongly influenced by cold extremes in the early period and by warm extremes in the late period. As a sensitivity analysis, we reran Models 2 and 3 using total pollock CPUE data (all body lengths combined) over a limited range of observed bottom temperatures that excluded the coldest and warmest temperatures to maximize the extent of overlap between periods. Because warm temperatures were relatively rare in the colder 1982–2013 period, we removed (from both periods) observations that were warmer than the 95th warmest percentile of temperatures observed in the early period (i.e. temperatures warmer than 4.8°C). Likewise, we removed temperatures colder than the 5th coldest percentile of temperatures observed in the warm late period (i.e. temperatures colder than 0.0°C). This filtering approach resulted in 79.7% of observations (11 159 observations out of 14 006) being retained in the new limited dataset. These percentiles for filtering were chosen somewhat subjectively, as our goal was simply to remove extreme observations and rerun our models to check for potential bias caused by these extremes. All other model aspects were held the same.

We conducted further sensitivity analyses using total pollock CPUE to address uncertainties due to our *a priori* choice of a breakpoint between 2013 and 2014 and due to the limited number of years available for analysis since the warming trend began around 2014. First, to determine whether the selected breakpoint was appropriate, we re-fit the 2 models with period interactions (Models 2 and 3) for every potential breakpoint with at least 6 years of data on either side (before/after). We compared AIC across these models to determine whether a better breakpoint could be identified. Second, to determine whether having only 6 years of data in 1 period impacts model choice, we re-fit Models 2 and 3 for every potential breakpoint using only 6 years of data for the late period. For example, for breakpoint 2000, the early period would include years 1982–1999, while the late period would include years 2000–2005. We then as-

sessed whether our choice of breakpoint affected how often the non-stationary models (Models 2 and 3) were selected over the non-linear model (Model 1) based on AIC.

Finally, to assess the ability of models fit to data from the SEBS to predict pollock CPUE in the NEBS (Objective 2), we used the best model for the SEBS along with observed temperatures and depths from NEBS surveys to predict CPUE in the NEBS for any years for which survey data were available (1982, 1985, 1988, 1991, 2010, 2017–2019, 2021). Predictions for a given year were done with random effects set to their predicted value for a given year, which assumes that year-specific deviations in mean CPUE estimated for the SEBS also apply to the NEBS. Predicted patterns in CPUE were compared visually to the observed CPUE in these years by plotting them through space and by fitting a linear model to the observed vs. predicted CPUE. If the slope of the linear model is similar to the slope of a 1:1 line, we interpreted that the model preforms similarly well at different catch levels. Prediction skill was compared among years using RMSE.

2.5.1. CPUE by length

To assess possible variation in the response of younger and older pollock to temperatures, we re-fit the CPUE models described above separately for selected body length classes. The CPUE for each length class was estimated by apportioning catches based on random subsamples of pollock caught in a given haul that were measured to the nearest centimeter of fork length. Pollock CPUE within each of 5 length bins was computed following Thorson et al. (2017): 0–20, 20–30, 30–40, 40–50, and >50 cm. Distributions of residuals are provided in Figs. S2–S6.

2.5.2. Community

We tested for non-stationarity in the spatial association between pollock and other species by comparing the extent to which pollock were correlated with that species through space in the early versus late period. For each year, we calculated an annual Pearson correlation coefficient between station-specific pollock CPUE and the CPUE of each other species across the SEBS. We used a separate *t*-test for each species to ask whether the mean correlation between pollock and that species differed between the early and late periods, assuming that each year within a period provides an independent estimate of the between-species association for that period.

Because we conducted multiple tests (9 *t*-tests in total), we controlled the false discovery rate (FDR) following the procedure proposed by Benjamini & Hochberg (1995) (Verhoeven et al. 2005). Our null hypothesis for each test was that there was no difference in correlation between species in the early versus late period. For each of the m tests, p-values were ranked in ascending order (P_i, where i is ranked order) and all null hypotheses for which $P_i \leqslant \frac{\alpha}{m} i$ were rejected.

All statistical analyses were performed using R version 4.1.2 (R Core Team 2021). Models described in Section 2.4 were fit and missing values were predicted using the mgcv package (Wood 2011, 2017). All CPUE models described in Section 2.5 were fit using the gamm() function in package mgcv (Wood 2017). Correlations were examined using the cor() function in R (R Core Team 2021). Figures were created using packages ggplot2 (see our Figs. 1, 4, 5, & 7; Wickham 2009), rnaturalearth (see our Figs. 1 & 4; South 2017), itsadug (see our Fig. 2A,B; van Rij et al. 2020), mgcViz (see our Fig. 2C; Fasiolo et al. 2020), and gratia (see our Figs. 3 & 6; Simpson 2022). Code used to perform analyses and create figures for this study is publicly available at: https://github.com/KristaOke/bold-new-pollock-CPUE.

3. RESULTS

3.1. Pollock CPUE

Our first objective was to determine whether the relationship between local pollock abundance and bottom temperature in the SEBS has changed in the warm 2014–2019 period relative to the 1982–2013 period. Pollock CPUE data were best fit by the model that allowed for a time-varying response to bottom temperature (Model 4, Table 1). This result suggests that there has been a slow shift in the bottom temperature–local pollock abundance relationship through time. The time-varying effect of bottom temperature was similar to the single smoothed effect of temperature (Model 1), which was dome-shaped, with low CPUE at temperatures below 0°C, rising to a maximum around 2°C, and declining again beyond temperatures of 4°C (Fig. 2). Few measurements at very high temperatures contributed to high uncertainty above temperatures of 8°C. The key difference between Models 1 and 4 was that the time-varying effect in Model 4 showed a shift beginning around 2010 towards higher CPUEs

Table 1. Comparison of model fit for the 4 alternative models compared for Objective 1. AIC: Akaike information criterion; RMSE: root mean square error from leave-one-out cross validation

Model	R^2	AIC	ΔAIC	Akaike weight	RMSE	Effect of depth	Temperature term	Effect of temperature
Model 1: non-linear	0.299	45605.88	20.41	0	1.52	$F = 91.62$, $p < 0.0001$	Main effect	$F = 78.80$, $p < 0.0001$
Model 2: non-stationary non-linear	0.300	45612.97	27.50	0	1.52	$F = 92.294$, $p < 0.0001$	Factor smoothed interaction	Early: $F = 78.407$, $p < 2 \times 10^{-16}$ Late: $F = 7.918$, $p < 0.0001$
Model 3: non-stationary linear	0.205	46077.07	491.6	0	1.62	$F = 110.8$, $p < 0.0001$	Interaction	$F = 36.48$, $p < 0.0001$
Model 4: time-varying	0.320	45585.46	0	1	1.51	$F = 92.40$, $p < 0.0001$	Time varying	$F = 17.759$, $p < 0.0001$ (interaction with year)

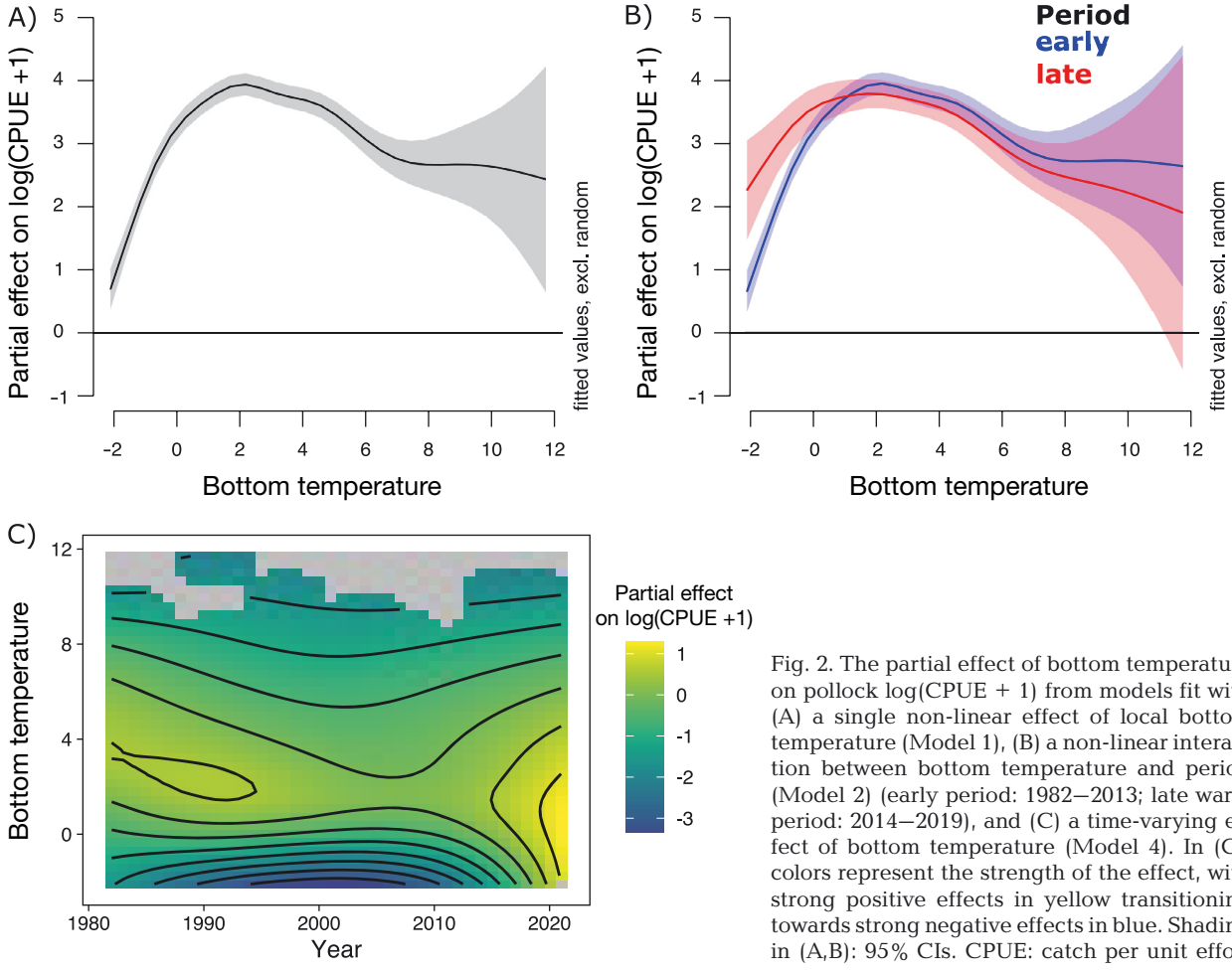

Fig. 2. The partial effect of bottom temperature on pollock log(CPUE + 1) from models fit with (A) a single non-linear effect of local bottom temperature (Model 1), (B) a non-linear interaction between bottom temperature and period (Model 2) (early period: 1982–2013; late warm period: 2014–2019), and (C) a time-varying effect of bottom temperature (Model 4). In (C), colors represent the strength of the effect, with strong positive effects in yellow transitioning towards strong negative effects in blue. Shading in (A,B): 95% CIs. CPUE: catch per unit effort

at cold bottom temperatures. The next best fit was provided by the model that allowed the non-linear effect of bottom temperature on CPUE to differ between periods (Model 2), but the shapes of the 1982–2013 and 2014–2019 smoothers were similar both to one another and to the single smoother from Model 1. Similar to Model 4, cold temperatures had a less negative effect on log(CPUE + 1) in the late period, while warm temperatures had a more negative effect, compared to the 1982–2013 period. The model with a linear bottom temperature–period interaction (Model 3) provided the worst fit.

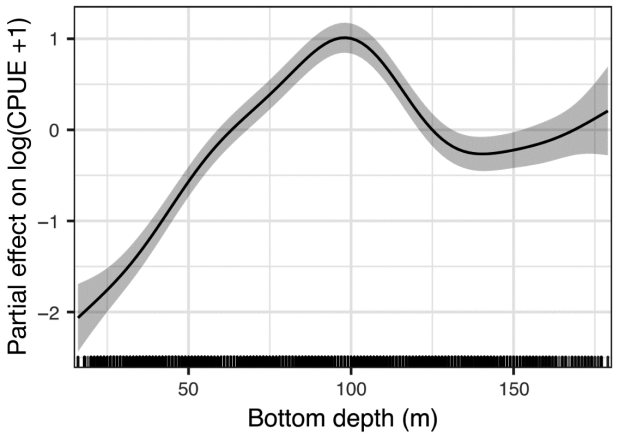

Fig. 3. The partial effect of bottom depth on eastern Bering Sea pollock catch per unit effort (log(CPUE + 1)) from models with a single, non-linear response to local bottom temperature (Model 1). Shading: 95% CIs

In all models, bottom depth had a significant non-linear effect on CPUE (Table 1). For all 4 models (Fig. 3), CPUE increased with increasing depth from 0 to 100 m then decreased between depths of about 100–130 m. Beyond about 130 m, uncertainty increased as the effect on CPUE became slightly more positive. Given that the effect of bottom depth was very similar across models and because we include it primarily to account for the known effect of bottom depth on pollock CPUE, we focus the rest of the paper on the results for temperature effects that address the main goals of our study.

Our second objective was to assess the ability of models of local pollock abundance fit to data from the SEBS to predict pollock abundance in the NEBS. Out-of-sample predictions of pollock CPUE generally captured relative spatial patterns in CPUE in the

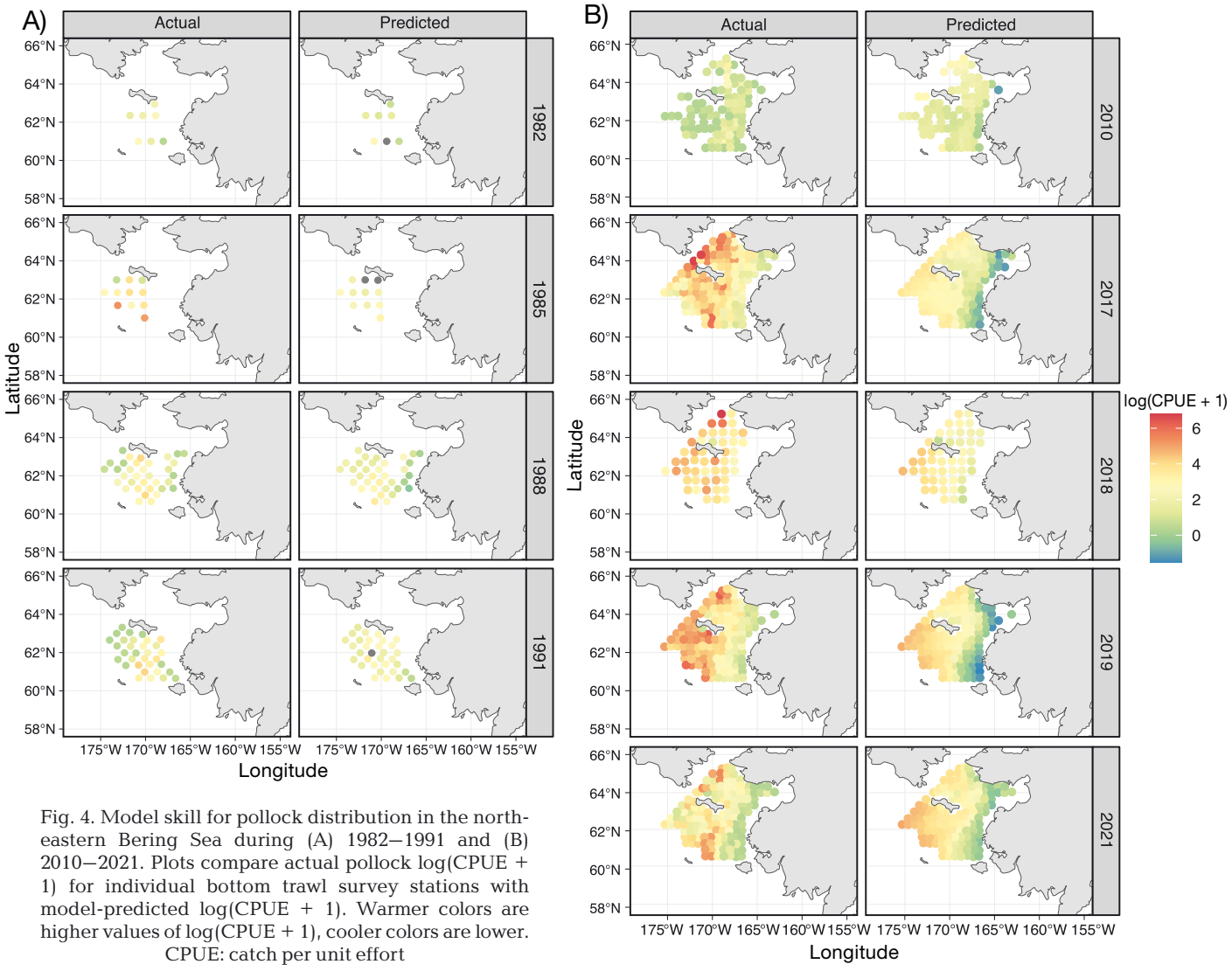

Fig. 4. Model skill for pollock distribution in the northeastern Bering Sea during (A) 1982–1991 and (B) 2010–2021. Plots compare actual pollock log(CPUE + 1) for individual bottom trawl survey stations with model-predicted log(CPUE + 1). Warmer colors are higher values of log(CPUE + 1), cooler colors are lower. CPUE: catch per unit effort

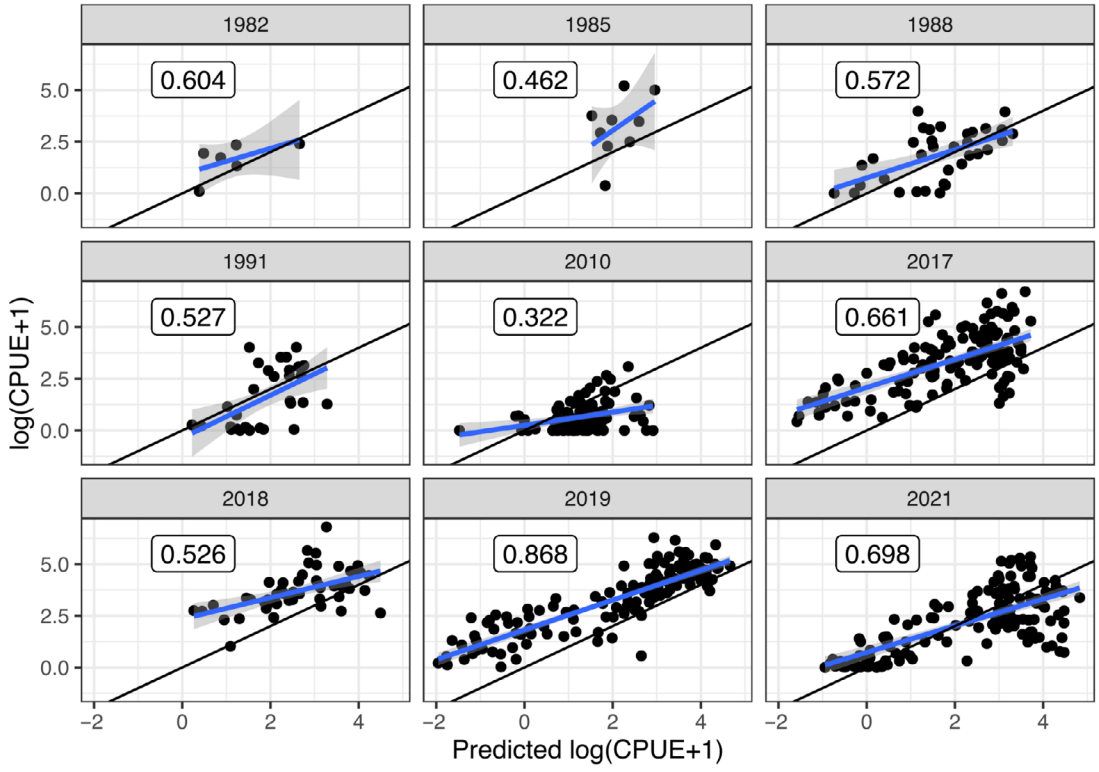

Fig. 5. 1:1 plot comparing actual catch per unit effort (log(CPUE + 1)) on the *y*-axis with model-predicted CPUE on the *x*-axis. Points that fall along the 1:1 line (black line) show good agreement between predicted and actual results, whereas points that fall above the 1:1 line had higher actual CPUE than the model predicted, and vice versa. The further an individual point is from the 1:1 line, the worse the agreement between predicted and actual catch for that sampling point. We also fit a linear model (blue) to the observed vs. predicted to aid in interpretation. If the slope of the linear model is similar to the slope of the 1:1 line, we would interpret that the model preforms similarly well at different catch levels. Years with linear model fits that fall entirely above the 1:1 line represent years with generally higher catch than predicted, and vice versa. Boxed numbers: correlations between predicted and observed values for each year

NEBS, although not in all areas in all years (Fig. 4). However, the model did a poor job predicting the magnitude of catches in the NEBS in recent years. The model overestimated CPUE in the NEBS in 2010, whereas in 2017–2019 and to some extent in 2021, the model strongly underpredicted CPUE (Fig. 5). RMSE for each year was generally lower in earlier or cooler years ($RMSE_{1982}$ = 0.844, $RMSE_{1988}$ = 1.08, $RMSE_{1991}$ = 1.23, $RMSE_{2010}$ = 1.03), except 1985 ($RMSE_{1985}$ = 1.66), and higher in the warm late 2010s ($RMSE_{2017}$ = 1.87, $RMSE_{2018}$ = 1.44, $RMSE_{2019}$ = 1.56, and $RMSE_{2021}$ = 1.23), although late years tended to have higher correlations among predicted and observed CPUE (Fig. 5). In short, the model built on data from the SEBS successfully predicted where high and low CPUE would occur in the NEBS, but overestimated CPUE in cold years and underestimated CPUE in warm years.

The sensitivity tests supported the results from the models discussed above. Results based on a subset of the data spanning a narrower temperature range were generally consistent with those based on the entire dataset. The time-varying model (Model 4) provided the best fit, followed by the nonlinear model (Model 1, ΔAIC = 25.5), and the estimated effects of bottom temperature were very similar to the effects estimated for the entire dataset. Rerunning the linear interaction model with all possible breakpoints generally did not identify a better breakpoint than 2014 (i.e. most potential breakpoints were not better than 2014 by ΔAIC of 4 or more), with 1 interesting exception. The best breakpoint identified was 1988 (ΔAIC = −19.4 relative to the model without a breakpoint), and 1989 (ΔAIC = −9.55), 1990 (ΔAIC = −13.2), 1991 (ΔAIC = −7.52), and 2012 (ΔAIC = −2.62) were also better than 2014 (ΔAIC = 7.09). When including only 6 years of data after each breakpoint, only 1988 (ΔAIC = −12.0) was meaningfully better than 2014. The 1988 and 1989 breakpoints correspond to a well-documented regime shift

in the North Pacific. While it is beyond the scope of our project, future work investigating possible non-stationarity in the bottom temperature–pollock CPUE relationship surrounding the 1988/89 event might be fruitful.

3.2. Pollock CPUE by length

Our third objective was to determine whether the local abundances of different size classes responded differently to warm temperatures in the warm 2014–2019 period. As was the case for the overall CPUE model, CPUE by size class (5 length bins) was generally best fit by models that included a time-varying effect of bottom temperature (Table 2, Fig. 6). Data from the smallest size bin (0–20 cm) were better fit by a single, dome-shaped effect of temperature (Model 1). Data from the largest size bin (>50 cm) were similarly well fit by either a temperature-by-period interaction (Model 2) or a temperature-by-year interaction (Model 4, ΔAIC = 0.284), favoring the more parsimonious Model 2. Overall, the response to temperature was similar across size classes, though perhaps slightly different for the smallest and largest size bins.

CPUE within the preferred temperature range was generally higher for the larger length bins, as would be expected given that the bottom trawl survey has a higher selectivity for larger fish and more biomass accumulates in the larger length bins. In addition, the dome shape of the bottom temperature term became much more pronounced as body size increases, suggesting that larger fish have a stronger affinity for or a better capacity to stay within a preferred temperature range. These results, along with the fact that the models for the largest length bins were more similar to the overall (all size classes) model than were those for the smaller length bins, suggest that the overall response to temperature is largely being driven by fish larger than 40 cm.

Table 2. Comparison of model fit for the alternative models for each length bin compared for Objective 3. Models compared include the non-linear (Model 1), non-stationary non-linear model (Model 2), non-stationary linear (Model 3), and time varying (Model 4) models. AIC: Akaike information criterion

Length bin (cm)	Model	R^2	AIC	ΔAIC	Akaike weight
0–20	1	0.048	12015.86	0	0.975
	2	0.049	12023.77	7.91	0.019
	3	0.025	12071.42	55.6	0
	4	0.055	12026.02	10.2	0.006
20–30	1	0.116	18596.10	34.5	0
	2	0.119	18564.16	2.60	0.215
	3	0.071	18728.21	167	0
	4	0.149	18561.56	0	0.785
30–40	1	0.211	35191.85	70.0	0
	2	0.212	35137.65	15.8	0
	3	0.179	35330.45	209	0
	4	0.242	35121.83	0	1.0
40–50	1	0.347	42406.94	106	0
	2	0.341	42323.57	22.9	0
	3	0.256	42627.21	327	0
	4	0.399	42300.63	0	1
>50	1	0.183	39314.40	51.6	0
	2	0.189	39262.77	0	0.536
	3	0.104	39762.26	499	0
	4	0.210	39263.05	0.284	0.464

3.3. Community

To address our fourth objective (to evaluate the evidence for non-stationarity in the spatial association between the abundance of pollock and other common species), we compared the extent of spatial association between pollock and other species in the early and late periods (Fig. 7). After controlling for the FDR to account for multiple tests, 3 of 9 species showed a significantly different correlation with pollock in the early versus late period: Alaska plaice ($t_{20.2} = -5.33$, $p = 3.15 \times 10^{-5}$), Tanner crab ($t_{7.08} = 3.22$, $p = 0.014$), and Pacific halibut ($t_{9.00} = 2.95$, $p = 0.016$). A weakly negative correlation (mean = −0.08) between plaice and pollock in the early period shifted to a weak positive correlation (mean = 0.13) in the late period, whereas a weakly negative correlation between halibut and pollock in the early period (mean = −0.072) became more negative in the late period (mean = −0.238). The positive correlation between Tanner crab and pollock (mean = 0.173) disappeared in the late period (mean = −0.068). Correlations between pollock and the other 6 species did not differ significantly between periods. Overall, there appears to be some evidence that the magnitude and/or sign of spatial associations between pollock and some other common SEBS species has changed, reflecting an increased association with a more northern species (Alaska plaice) and weaker associations with 2 more southern species (halibut and Tanner crab) in the 2014–2019 warm period.

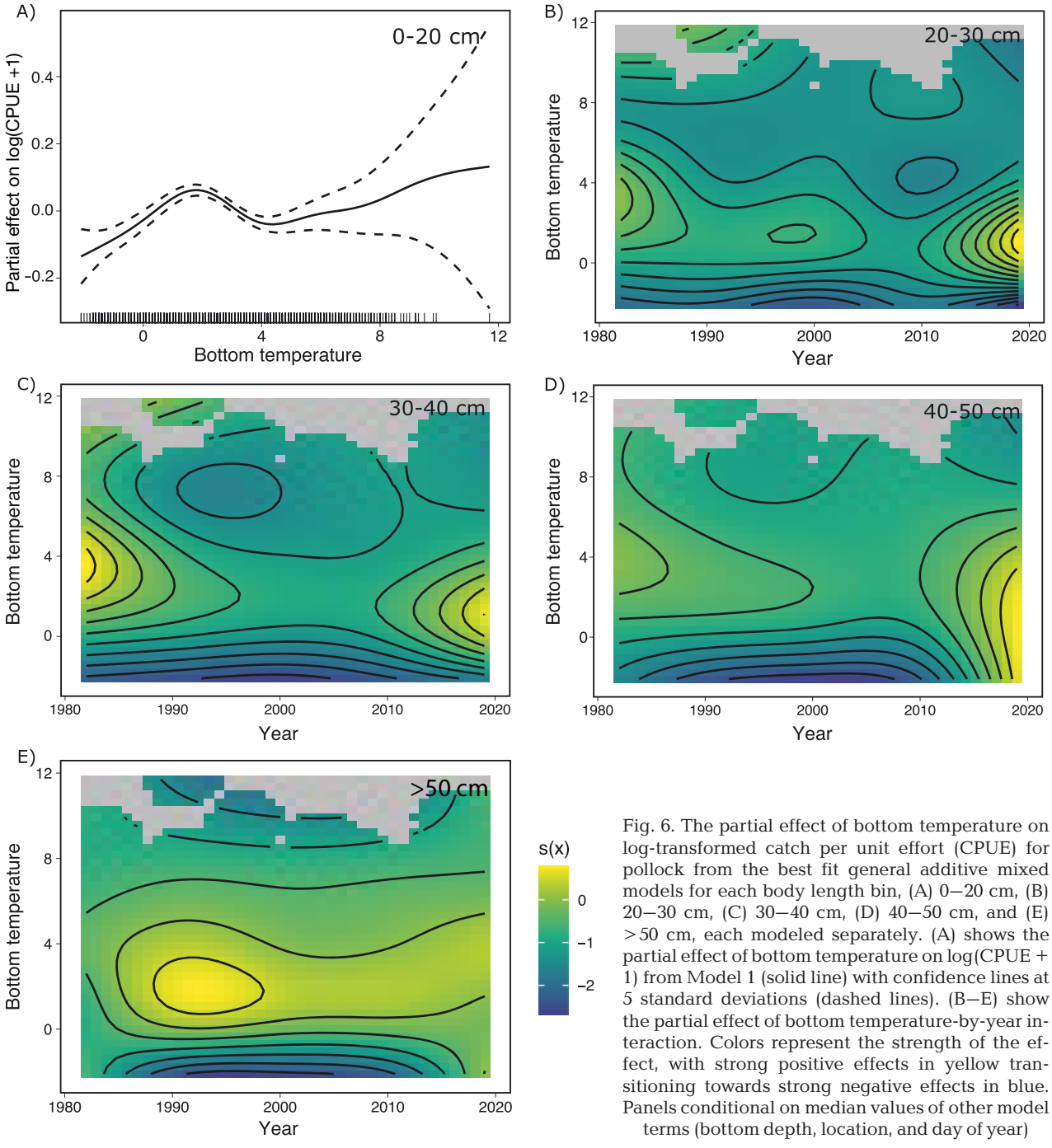

Fig. 6. The partial effect of bottom temperature on log-transformed catch per unit effort (CPUE) for pollock from the best fit general additive mixed models for each body length bin, (A) 0–20 cm, (B) 20–30 cm, (C) 30–40 cm, (D) 40–50 cm, and (E) >50 cm, each modeled separately. (A) shows the partial effect of bottom temperature on log(CPUE + 1) from Model 1 (solid line) with confidence lines at 5 standard deviations (dashed lines). (B–E) show the partial effect of bottom temperature-by-year interaction. Colors represent the strength of the effect, with strong positive effects in yellow transitioning towards strong negative effects in blue. Panels conditional on median values of other model terms (bottom depth, location, and day of year)

4. DISCUSSION

The relationship between local bottom temperature and pollock CPUE through time has shifted significantly but subtly through time. The bottom temperature–local abundance relationship was generally dome-shaped, with both very high and very low temperatures correlating with low CPUE (Fig. 2). Pollock CPUE data were best fit by a time-varying model (Model 4, Fig. 2C), but the change through time was a gradual shift towards less negative impacts of cold temperatures later in the time series rather than a sharp transition. This model, developed based on data for the SEBS, had some predictive skill in the NEBS, capturing general spatial patterns of CPUE but underpredicting CPUE during warm years. In addition, ev-

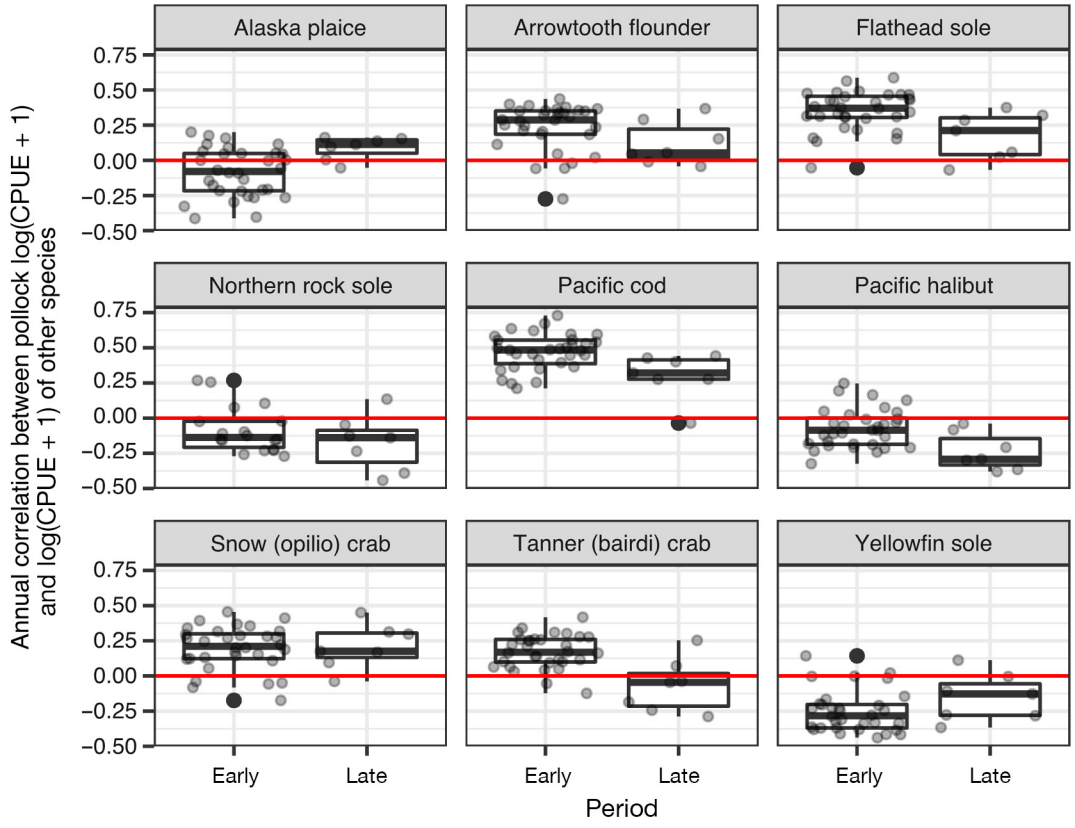

Fig. 7. Distribution of within-year correlations between pollock and other Bering Sea species across sampling stations plotted for early vs. late period to visualize whether the extent of correlation in log(CPUE + 1) between pollock and other species has changed. The correlations differed significantly between periods for 3 comparisons: pollock and Alaska plaice, pollock and Pacific halibut, and pollock and Tanner crab. Smaller grey points: annual correlations, jittered for visibility; larger black points: boxplot outliers. The zero line (red) would indicate no correlation between pollock and the other species; points falling above (below) the zero line indicate positive (negative) correlations. Thick center line on each box: median; upper and lower hinges: first and third quartiles; whiskers: the largest (upper) or smallest (lower) value at least 1.5 × the interquartile range. CPUE: catch per unit effort

idence was limited that recent warm temperatures revealed non-stationarity in community interactions, given that the extent of spatial correlation between pollock and several prey, predator, and competitor species was significantly different following the onset of warm conditions in 2014 in only 3 of 9 cases (Alaska plaice, Tanner crab, and Pacific halibut). Overall, our results suggest that although climate and species distributions have changed rapidly in the EBS, there is limited evidence for non-stationary relationships between pollock and temperature, or in associations between pollock and other common demersal species.

4.1. Pollock CPUE

Across models, there was generally a dome-shaped effect of bottom temperature, with CPUE increasing with increasing temperature to a certain point, beyond which warmer temperatures resulted in declining CPUE. This result is not surprising, given extensive evidence that species have thermal performance curves that influence organismal performance and fitness (Kingsolver 2009). The best fit model (Model 4, Fig. 2C) showed the dome shape changing though time, with later (2014–2019) warm years showing a lower magnitude negative impact of cold temperatures on CPUE. Cooler temperatures were observed less frequently during the later warm years, but were generally associated with higher CPUE. Together with recent documentation of dramatic northward shifts in the distribution of pollock (Stevenson & Lauth 2019, Eisner et al. 2020, O'Leary et al. 2020), our results suggest that temperatures in the EBS during the warm 2014–2019 period could have exceeded pollock's thermal optimum, causing them to seek out areas of cooler water or avoid areas of warm water by moving northward during summer. Range shifts in response to changing climate have been widely documented (Parmesan & Yohe 2003, Perry et al. 2005,

Pinsky et al. 2020) and present a major challenge for fisheries management (Cheung 2018).

The weaker support for temperature effects interacting with period suggests that the exceptionally warm conditions that occurred beginning in 2014 were not associated with a sharp transition in the relationship between local pollock abundance and temperature. From a practical standpoint, our results suggest that accounting for potential temporal non-stationarity in pollock–temperature relationships in the Bering Sea might not be of high priority. Several recent studies on pollock have included dome-shaped relationships with temperature (e.g. Thorson et al. 2017, Grüss et al. 2020). While our results suggest that this relationship has shifted over the range of temperature conditions that have been observed to date, it does not appear to have undergone any sharp transitions that might lead to major breakdowns in predictive ability. However, allowing these dome-shaped temperature relationships to change through time might be prudent, especially if the relationship continues to change in future climate conditions.

A potential concern as pollock shift their distribution into new habitats in the NEBS is that patterns in their local abundance could differ in response to novel environmental conditions or community interactions found in the NEBS but not in the SEBS. It was encouraging that the model parameterized for the SEBS did have predictive skill in the NEBS. The model was able to generally identify areas of high or low CPUE during the warm period in the NEBS (Fig. 4), although predictions tended to underestimate CPUE compared to actual observations from 2017–2019 and in 2021 and to overestimate CPUE in 2010. Pollock tend to aggregate along the edges of the cold pool at 2°C (Kotwicki et al. 2005), as evident in a peak in CPUE (Fig. 2), but clearly tolerate cooler waters with relatively high densities extending into the cold pool in at least some years (Ianelli et al 2020). However, the extensive cold pool in 2010 (Kotwicki & Lauth 2013) may have limited summer feeding migrations into the northern Bering Sea. In contrast, the cold pool was much smaller or absent during the warm years from 2017–2019 and 2021, promoting the northward migration of pollock to stay within their preferred temperature range. Pollock CPUE in the NEBS in these years may have been higher than predicted because a large proportion of the EBS pollock population shifted northward (Stevenson & Lauth 2019), presumably to avoid warm temperatures on the southern shelf. The surface area of the NEBS shelf is smaller than that of the SEBS, which could have resulted in higher than predicted CPUE as pollock crowded into more favorable habitats over a relatively smaller area on the NEBS shelf. Taken together, it appears that the environmental factors that control pollock local abundances and distribution in the SEBS generally hold in the NEBS and will be useful covariates in modeling future pollock distribution throughout, and potentially beyond, the current SEBS–NEBS survey area.

Other factors could contribute to the model's underestimation of CPUE in the NEBS during warm years. First, the NEBS and SEBS have different oceanographic features. Our model included a smoothed bottom depth term, which showed highest CPUE at depths around 100 m in the SEBS corresponding to a prominent frontal structure between 2 oceanographic domains (Aydin & Mueter 2007). The NEBS is generally shallower than the SEBS, with a maximum depth of about 80 m. It seems likely that the model could be failing to predict high CPUE because bottom depth is generally shallower than the optimal depths for pollock in the SEBS. Second, we set the year random effect to its predicted value when predicting NEBS CPUEs, which assumes year-specific deviations in mean CPUE estimates for the SEBS apply to the NEBS. However, we expect many or most of the pollock caught in the NEBS moved there from the SEBS. Thus, years of high catch in the NEBS are likely low catch years in the SEBS, which could partially explain why our model underpredicted the magnitude of CPUE in the NEBS. Third, our models were unable to include other variables that could influence pollock distributions, particularly the cold pool. Pollock avoid the cold pool (Kotwicki et al. 2005, Mueter & Litzow 2008, Kotwicki & Lauth 2013) and including indices that measure cold pool extent (annual or spatial) might improve future models' predictive ability in the NEBS. Finally, an unexplored consideration is that pollock have likely not only moved into the portion of the NEBS covered by NOAA survey efforts but also into the Russian portion of the NEBS (Eisner et al. 2020, O'Leary et al. 2022). While movement out of the survey area would not explain our model's tendency to underpredict local abundances in the NEBS, it will be an important consideration as pollock shift their distribution in response to warming.

4.2. Pollock CPUE by length

The strongly non-linear relationship between bottom temperature and pollock CPUE appears to be largely driven by fish greater than 40 cm, which have higher CPUE by biomass in the bottom trawl survey

than smaller pollock. Indeed, caution is likely warranted in interpreting results for the smallest size classes, whose distribution may not be well represented by the bottom trawl survey due to gear selectivity and because of their greater tendency to occur off bottom compared to larger fish (Kotwicki et al. 2015). Overall, length classes differed primarily in the amplitude of the response — the CPUE of all length classes peaked around 2°C and decreased at colder or warmer conditions (Fig. 6) — rather than a fundamental difference in the shape of the response among size classes. These consistent relationships across size classes contrast with a recent study that shows age-specific impacts of sea surface temperature (SST) on EBS pollock weight-at-age (Oke et al. 2022).

4.3. Community

Species do not respond to climate change in a vacuum. Different species respond differently to climate change, leading to shifts in community dynamics, including new predator–prey interactions, mis-matches between predators and prey, and changes in competition (Williams & Jackson 2007, Urban et al. 2012). We expected that the northward movement of many species from the SEBS into the NEBS (Stevenson & Lauth 2019, O'Leary et al. 2020) might result in different spatial associations between pollock and other species in the late (post-2014) period compared to the relatively cooler earlier period, with implications for pollock CPUE.

Contrary to expectations, we found that spatial associations between pollock and other species changed significantly between the early and late period in only 3 of 9 comparisons (Alaska plaice, Tanner crab, and Pacific halibut; Fig. 7). However, our ability to detect such shifts could be limited by the relatively few years of observation in the warm 2014–2019 period. Mean correlations between the local abundances of species across space were typically weak to moderate ($|r|$ from 0 to 0.5). One exception was the moderately strong positive correlation between pollock and Pacific cod (mean: $r = 0.47$ in early period), which ranged from 0.21 to 0.72 in all but 1 year, suggesting similar habitat requirements or similar responses to dynamic environmental drivers across both periods. Interestingly, the only year that Pacific cod and pollock were not strongly correlated was 2014, the first year in the warm 2014–2019 period, suggesting the possibility that one species could have shifted into the NEBS faster than the other, leading to a disconnect between their spatial distributions in the SEBS. The lack of a survey in the NEBS in 2014 makes this hypothesis difficult to test. We did not investigate the dynamics of other prey communities, such as zooplankton, which are the main prey of smaller pollock and could therefore be important, especially given the sometimes strong bottom-up control on pollock recruitment predicted by the oscillating control hypothesis (Hunt et al. 2002, 2011, Mueter et al. 2006). However, observations of high pollock condition during warm years (Boldt et al. 2015), including 2016–2019 (Grüss et al. 2020, 2021), suggest that prey is generally not limiting.

The weak evidence for non-stationarity in pollock–temperature relationships and limited evidence for non-stationary pollock–community relationships in the EBS contrasts with extensive evidence for stark shifts or breakdowns in climate–biology and climate–climate relationships in the Gulf of Alaska associated with a 1988–1989 regime shift. Non-stationary relationships with major climate indices have been detected for many North Pacific species (Litzow et al. 2018, 2019, 2020a,b, Puerta et al. 2019), including pollock (Litzow et al. 2019, Puerta et al. 2019). However, even in systems like the Gulf of Alaska where non-stationarity is common, not all fishes show non-stationary climate–biology relationships. Of the 9 species investigated by Puerta et al. (2019), herring *Clupea pallasii*, sablefish *Anoplopoma fimbria*, and arrowtooth flounder *Atheresthes stomias* all showed stationary relationships between productivity and SST across the 1988–1989 regime shift. One possible explanation for the lack of non-stationarity detected in our analyses could be that, unlike the more commonly considered 1988/1989 regime shift, the effects of a putative shift in temperatures that started around 2014 were too recent to detect. In addition, future studies might better reveal the extent of non-stationarity (or lack thereof) using methods that consider community-level dynamics, rather than multiple comparisons of species pairs. We note that a lack of non-stationarity for pollock–temperature relationships in the SEBS does not imply that other climate–biology relationships are stationary across the 2014 shift.

4.4. Implications and conclusions

As ecological novelty increases, due to either novel climate conditions or species interactions, the predictability of population responses is generally expected to decrease (Radeloff et al. 2015), which could present a challenge for fisheries management. Efforts to include ecosystem information in management decision making and especially stock assessment

models must address the potential for non-stationarity in climate–biology relationships, which could lead to weakened model performance in the future. For example, well-documented environment–recruitment relationships are known to frequently break down when tested with new data (Myers 1998, McClatchie et al. 2010). For SEBS pollock, our results revealed mixed evidence for temporal non-stationarity under the climate conditions that have been observed to date, with little evidence of non-stationarity in pollock–community relationships, but a gradual shift in local pollock abundance–temperature relationships. This limited evidence for non-stationarity shows that non-stationary responses are not ubiquitous, even in the face of rapid climate change. As species shift their distributions in response to climate change, our study could provide a template for evaluations of the extent of non-stationarity in local abundance patterns to help scientists and managers understand whether species will be associated with similar habitat features in areas of newly expanded distributions. These sorts of evaluations will be important as assessment authors and management bodies work towards ecosystem-based fisheries management. Future work on pollock dynamics in the NEBS and the warming SEBS, as well as the dynamics of their predators, competitors, and prey, will help to determine the extent to which models parameterized for pollock dynamics in the SEBS can be extrapolated into the NEBS and beyond as the Bering Strait region continues to change.

Of course, our study considered several years of climate conditions that were considered highly improbable just a decade ago (Stabeno et al. 2012). What will happen to EBS climate in the next few decades remains to be seen, but further warming could still reveal non-stationary processes. Our results showed some mixed evidence for temporal non-stationarity, but overall suggest that temporal non-stationarity does not currently appear to be of high concern for EBS pollock. Testing for non-stationarity could help identify other circumstances or stocks for which climate–biology relationships have been either largely stable or shifted in ways that can be relatively easily accounted for statistically, which would encourage and facilitate the incorporation of environmental variables into the stock assessment process. As the North Pacific enters novel climate conditions, non-stationarity could be common but not ubiquitous, or could be delayed for certain areas or processes. Future investigations of climate–climate and climate–biology relationships will help determine the extent to which non-stationarity does or does not complicate our understanding of ecosystem dynamics in the EBS.

Acknowledgements. We thank J. Thorson, C. Cunningham, and C. O'Leary for helpful discussions. We are very grateful to the individuals and agencies who collected the data used in the current paper, especially those who have contributed to the collection and curation of the NOAA bottom trawl survey data which formed the basis for our study. We thank the editors and 3 reviewers for helpful comments that improved the paper. Work on this paper was conducted on Alutiiq/Sugpiaq land home to the Sun'aq Tribe of Kodiak and on Lingít Aaní home to the Áak'w Kwáan. Funding for this project was provided by the Pollock Conservation Cooperative Research Center (PCCRC Project #19-02) and NOAA through the Saltonstall-Kennedy Grant Program (award #NA18NMF 4270202).

LITERATURE CITED

Alabia ID, Molinos JG, Hirawake SST, Hirata T, Mueter FJ (2018) Distribution shifts of marine taxa in the Pacific Arctic under contemporary climate changes. Divers Distrib 24:1583–1597

Araujo MB, New M (2006) Ensemble forecasting of species distributions. Trends Ecol Evol 22:42–47

Aydin K, Mueter F (2007) The Bering Sea — a dynamic food web perspective. Deep Sea Res II 54:2501–2525

Benjamini Y, Hochberg Y (1995) Controlling the false discovery rate: a practical and powerful approach to multiple testing. J R Stat Soc 57:289–300

Boldt J, Rooper C, Hoff J (2015) Eastern Bering Sea groundfish condition. In: Zador S (ed) Ecosystem considerations 2015: status of Alaska's marine ecosystems. North Pacific Fishery Management Council, Anchorage, AK, p 182–190

Brown JH, Gillooly JF, Allen AP, Savage VM, West GB (2004) Toward a metabolic theory of ecology. Ecology 85: 1771–1789

Burnham KP, Anderson DR (2002) Model selection and multimodel inference: a practical information-theoretic approach. Springer, New York, NY

Cheung WWL (2018) The future of fishes and fisheries in the changing oceans. J Fish Biol 92:790–803

Ciannelli L, Brodeur RD, Swartzman GL, Salo S (2002) Physical and biological factors influencing the spatial distribution of age-0 walleye pollock (*Theragra chalcogramma*) around the Pribilof Islands, Bering Sea. Deep Sea Res II 49:6109–6126

Cote J, Brodin T, Fogarty S, Sih A (2017) Non-random dispersal mediates invader impacts on the invertebrate community. J Anim Ecol 86:1298–1307

Danielson SL, Ahkinga O, Ashjian C, Basyuk E and others (2020) Manifestation and consequences of warming and altered heat fluxes over the Bering and Chukchi Sea continental shelves. Deep Sea Res II 177:104781

Di Lorenzo E, Mantua N (2016) Multi-year persistence of the 2014/2015 North Pacific marine heatwave. Nat Clim Change 6:1042–1048

Duffy-Anderson JT, Stabeno P, Andrews AGI, Cieciel K and others (2019) Responses of the Northern Bering Sea and Southeastern Bering Sea pelagic ecosystems following record-breaking low winter sea ice. Geophys Res Lett 46: 9833–9842

Eisner LB, Zuenko YI, Basyuk EO, Britt LL and others (2020) Environmental impacts on walleye pollock (*Gadus chalcogrammus*) distribution across the Bering Sea shelf. Deep Sea Res II 181:104881

FAO (Food and Agriculture Organization of the United Nations) (2023) Fishery and aquaculture statistics — yearbook 2020. FAO yearbook of fishery and aquaculture statistics. FAO, Rome

Fasiolo M, Nedellec R, Goude Y, Wood SN (2020) Scalable visualization methods for modern generalized additive models. J Comput Graph Stat 29:78–86

Fitzpatrick MC, Hargrove WW (2009) The projection of species distribution models and the problem of non-analog climate. Biodivers Conserv 18:2255–2261

Frölicher TL, Fischer EM, Gruber N (2018) Marine heatwaves under global warming. Nature 560:360–364

Grebmeier JM, Overland JE, Moore SE, Farley EV and others (2006) A major ecosystem shift in the Northern Bering Sea. Science 311:1461–1464

Grüss A, Gao J, Thorson JT, Rooper CN, Thompson G, Boldt JL, Lauth R (2020) Estimating synchronous changes in condition and density in eastern Bering Sea fishes. Mar Ecol Prog Ser 635:169–185

Grüss A, Thorson JT, Stawitz CC, Reum JCP, Rohan SK, Barnes CL (2021) Synthesis of interannual variability in spatial demographic processes supports the strong influence of cold-pool extent on eastern Bering Sea walleye pollock (*Gadus chalcogrammus*). Prog Oceanogr 194:102569

Hunsicker ME, Ciannelli L, Bailey KM, Zador S, Stige LC (2013) Climate and demography dictate the strength of predator–prey overlap in a subarctic marine ecosystem. PLOS ONE 8:e66025

Hunt GL, Stabeno P, Walters G, Sinclair E, Brodeur RD, Napp JM, Bond NA (2002) Climate change and control of the southeastern Bering Sea pelagic ecosystem. Deep Sea Res II 49:5821–5853

Hunt GLJ, Coyle KO, Eisner LB, Farley EV and others (2011) Climate impacts on eastern Bering Sea foodwebs: a synthesis of new data and an assessment of the Oscillating Control Hypothesis. ICES J Mar Sci 68:1230–1243

Huntington HP, Danielson SL, Wiese FK, Baker M and others (2020) Evidence suggests potential transformation of the Pacific Arctic ecosystem is underway. Nat Clim Change 10:342–348

Ianelli J, Kotwicki S, Honkalehto T, Holsman K, Fissel B (2018) Chapter 1: Assessment of the walleye pollock stock in the Eastern Bering Sea. NPFMC Bering Sea and Aleutian Islands SAFE Report. North Pacific Fishery Management Council, Anchorage, AK

Ianelli J, Fissel B, Holsman K, De Robertis A and others (2020) Assessment of the walleye pollock stock in the Eastern Bering Sea. NPFMC Bering Sea and Aleutian Islands SAFE Report. North Pacific Fishery Management Council, Anchorage, AK

Kearney K (2021) Temperature data from the eastern Bering Sea continental shelf bottom trawl survey as used for hydrodynamic model validation and comparison. US Dep Commerce, NOAA Tech Memo NMFS-AFSC-415

Kingsolver JG (2009) The well-temperatured biologist (American Society of Naturalists presidential address). Am Nat 174:755–768

Kotwicki S, Lauth RR (2013) Detecting temporal trends and environmentally-driven changes in the spatial distribution of bottom fishes and crabs on the eastern Bering Sea shelf. Deep Sea Res II 94:231–243

Kotwicki S, Buckley TW, Honkalekto T, Walters G (2005) Variation in the distribution of walleye pollock (*Theragra chalcogramma*) with temperature and implications for seasonal migration. Fish Bull 103:574–587

Kotwicki S, Horne JK, Punt E, Ianelli JN (2015) Factors affecting the availability of walleye pollock to acoustic and bottom trawl survey gear. ICES J Mar Sci 72:1425–1439

Laufkötter C, Zscheischler J, Frölicher TL (2020) High-impact marine heatwaves attributable to human-induced global warming. Science 369:1621–1625

Lauth RR, Dawson EJ, Conner J (2019) Results of the 2017 eastern and northern Bering Sea continental shelf bottom trawl survey of groundfish and invertebrate fauna. US Dep Commerce, NOAA Tech Memo NMFS-AFSC-396

Litzow MA, Ciannelli L, Puerta P, Wettstein JJ, Rykaczewski RR, Opiekun M (2018) Non-stationary climate–salmon relationships in the Gulf of Alaska. Proc R Soc B 285: 20181855

Litzow MA, Ciannelli L, Puerta P, Wettstein JJ, Rykaczewski RR, Opiekun M (2019) Nonstationary environmental and community relationships in the North Pacific Ocean. Ecology 100:e02760

Litzow MA, Hunsicker ME, Ward EJ, Anderson SC and others (2020a) Evaluating ecosystem change as Gulf of Alaska temperature exceeds the limits of preindustrial variability. Prog Oceanogr 186:102393

Litzow MA, Malick MJ, Bond NA, Cunningham CJ (2020b) Quantifying a novel climate through changes in PDO-climate and PDO-salmon relationships. Geophys Res Lett 47:e2020GL087972

Marsh JM, Mueter FJ, Thorson JT, Britt L, Zador S (2020) Shifting fish distributions in the Bering Sea [in: Richter-Menge J, Druckenmiller ML (eds) State of the climate in 2019: the Arctic]. Bull Am Meteorol Soc 101:S254–S256

McClatchie S, Goericke R, Auad G, Hill K (2010) Re-assessment of the stock–recruit and temperature–recruit relationships for Pacific sardine (*Sardinops sagax*). Can J Fish Aquat Sci 67:1782–1790

McIlroy D, Brownrigg R, Minka TP, Bivand R (2020) mapproj: map projections, version 1.2.7. https://cran.r-project.org/package=mapproj

Mueter FJ, Litzow MA (2008) Sea ice retreat alters the biogeography of the Bering Sea continental shelf. Ecol Appl 18:309–320

Mueter FJ, Ladd C, Palmer MC, Norcross BL (2006) Bottom-up and top-down controls of walleye pollock (*Theragra chalcogramma*) on the Eastern Bering Sea shelf. Prog Oceanogr 68:152–183

Myers RA (1998) When do environment–recruitment correlations work? Rev Fish Biol Fish 8:285–305

Oke KB, Mueter FJ, Litzow MA (2022) Warming leads to opposite patterns in weight-at-age for young versus old age classes of Bering Sea walleye pollock. Can J Fish Aquat Sci 79:1655–1666

O'Leary CA, Thorson JT, Ianelli JN, Kotwicki S (2020) Adapting to climate-driven distribution shifts using model-based indices and age composition from multiple surveys in the walleye pollock (*Gadus chalcogrammus*) stock assessment. Fish Oceanogr 29:541–557

O'Leary CA, DeFilippo LB, Thorson JT, Kotwicki S and others (2022) Understanding transboundary stocks' availability by combining multiple fisheries-independent surveys and oceanographic conditions in spatiotemporal models. ICES J Mar Sci 79:1063–1074

Oliver ECJ, Donat MG, Burrows MT, Moore PJ and others (2018) Longer and more frequent marine heatwaves over the past century. Nat Commun 9:1324

Parmesan C, Yohe G (2003) A globally coherent fingerprint

of climate change impacts across natural systems. Nature 421:37–42
Perry AL, Low PJ, Ellis JR, Reynolds JD (2005) Climate change and distribution shifts in marine fishes. Science 308:1912–1916
Pinsky ML, Selden RL, Kitchel ZJ (2020) Climate-driven shifts in marine species ranges: scaling from organisms to communities. Annu Rev Mar Sci 12:153–179
Puerta P, Ciannelli L, Rykaczewski RR, Opiekun M, Litzow MA (2019) Do Gulf of Alaska fish and crustacean populations show synchronous non-stationary responses to climate? Prog Oceanogr 175:161–170
R Core Team (2021) R: a language and environment for statistical computing. R Foundation for Statistical Computing, Vienna
Radeloff V, Williams JW, Bateman BL, Burke KD and others (2015) The rise of novelty in ecosystems. Ecol Appl 25: 2051–2068
Rohan SK, Barnett LAK, Charriere N (2022) Evaluating approaches to estimating mean temperatures and cold pool area from Alaska Fisheries Science Center bottom trawl surveys of the eastern Bering Sea. US Dep Commerce, NOAA Tech Memo NMFS-AFSC-456
Siddon EC, Kristiansen T, Mueter FJ, Holsman KK, Heintz RA, Farley EV (2013) Spatial match-mismatch between juvenile fish and prey provides a mechanism for recruitment variability across contrasting climate conditions in the eastern Bering Sea. PLOS ONE 8:e84526
Simpson GL (2022) gratia: graceful ggplot-based graphics and other functions for GAMs fitted using mgcv. https://cran.r-project.org/package=gratia
South A (2017) rnaturalearth: world map data from natural earth. https://cran.r-project.org/package=rnaturalearth
Spencer PD, Holsman KK, Zador S, Bond NA, Mueter FJ, Hollowed AB, Ianelli JN (2016) Modelling spatially dependent predation mortality of eastern Bering Sea walleye pollock, and its implications for stock dynamics under future climate scenarios. ICES J Mar Sci 73: 1330–1342
Stabeno PJ, Farley EV, Kachel NB, Moore S and others (2012) A comparison of the physics of the northern and southern shelves of the eastern Bering Sea and some implications for the ecosystem. Deep Sea Res II 65–70:14–30
Stevenson DE, Lauth RR (2019) Bottom trawl surveys in the northern Bering Sea indicate recent shifts in the distribution of marine species. Polar Biol 42:407–421
Thorson JT (2019) Measuring the impact of oceanographic indices on species distribution shifts: the spatially varying effect of cold-pool extent in the eastern Bering Sea. Limnol Oceanogr 64:2632–2645
Thorson JT, Ianelli J, Kotwicki S (2017) The relative influence of temperature and size structure on fish distribution shifts: a case study on walleye pollock in the Bering Sea. Fish Fish 18:1073–1084
Thorson JT, Fossheim M, Mueter FJ, Olsen E and others (2019) Comparison of near-bottom fish densities show rapid community and population shifts in Bering and Barents Seas. In: Richter-Menge J, Druckenmiller ML, Jeffries M (eds) Arctic Report Card 2019. NOAA, Silver Spring, MD, p 72–80. www.arctic.noaa.gov/Report-Card
Thorson JT, Arimitsu ML, Barnett LAK, Cheng W and others (2021) Forecasting community reassembly using climate-linked spatio-temporal ecosystem models. Ecography 44: 612–625
Uchiyama T, Mueter FJ, Kruse GH (2020) Multispecies biomass dynamics models reveal effects of ocean temperature on predation of juvenile pollock in the eastern Bering Sea. Fish Oceanogr 29:10–22
Urban MC, Tewksbury JJ, Sheldon KS (2012) On a collision course: Competition and dispersal differences create no-analogue communities and cause extinctions during climate change. Proc R Soc B 279:2072–2080
Urban MC, Bocedi G, Hendry AP, Mihoub JB and others (2016) Improving the forecast for biodiversity under climate change. Science 353:aad8466
van Rij J, Wieling M, Baayen R, van Rijn H (2020) itsadug: interpreting time series and autocorrelated data using GAMMs. https://cran.r-project.org/package=itsadug
Veloz SD, Williams JW, Blois JL, He F, Otto-Bliesner B, Liu Z (2012) No-analog climates and shifting realized niches during the late quaternary: implications for 21st-century predictions by species distribution models. Glob Change Biol 18:1698–1713
Verhoeven KJF, Simonsen KL, Mcintyre LM (2005) Implementing false discovery rate control: increasing your power. Oikos 108:643–647
Wainwright TC (2021) Ephemeral relationships in salmon forecasting: a cautionary tale. Prog Oceanogr 193:102522
Walsh JE, Johnson CM (1979) An analysis of Arctic Sea ice fluctuations, 1953–77. J Phys Oceanogr 9:580–591
Walsh JE, Thoman RL, Bhatt US, Bieniek PA and others (2018) The high latitude marine heat wave of 2016 and its impacts on Alaska. Bull Am Meteorol Soc 99:S39–S43
Wickham H (2009) ggplot2: elegant graphics for data analysis. Springer, New York, NY
Williams JW, Jackson ST (2007) Novel climates, no-analog communities, and ecological surprises. Front Ecol Environ 5:475–482
Wood SN (2011) Fast stable restricted maximum likelihood and marginal likelihood estimation of semiparametric generalized linear models. J R Stat Soc 73:3–36
Wood SN (2017) Generalized additive models: an introduction with R, 2nd edn. Chapman and Hall/CRC, New York, NY

Editorial responsibility: Konstantinos Stergiou, Thessaloniki, Greece
Reviewed by: C. O'Leary and 2 anonymous referees

Submitted: June 30, 2023
Accepted: September 23, 2024
Proofs received from author(s): November 1, 2024